Ionics (2015) 21:1461–1475
DOI 10.1007/s11581-014-1296-8

ORIGINAL PAPER

Methyl 3-((2-mercaptophenyl) imino) butanoate as an effective inhibitor against steel corrosion in HCl solution

G. Tansuğ · T. Tüken · G. Sığırcık · G. Fındıkkıran · E. S. Giray · M. Erbil

Received: 20 May 2014 / Revised: 9 October 2014 / Accepted: 22 October 2014 / Published online: 2 November 2014

Abstract Methyl 3-((2-mercaptophenyl) imino) butanoate (MMPB) was designed and synthesized as a corrosion inhibitor, which is functionalized with adjacent azole and thiol groups and a carboxylate tail. The inhibition efficiency of this compound has been investigated in different concentrations of HCl solutions. Then, the effect of temperature and inhibitor concentration was studied for further discussion about inhibition mechanism. In addition to potentiodynamic and electrochemical impedance spectroscopy, galvanic measurements were also realized for better explanation of interaction between inhibitor and metal surface. For this purpose, identical steel electrodes were immersed in separate test solutions with and without inhibitor, and then coupled to each other. The assessment of corrosion rate was realized with quantitative analysis of iron content in immersion test solutions. The corrosion current densities (i_{corr}) were 20.40 and 200.30 μA cm^{-2}, in the presence of 10 mM inhibitor and inhibitor-free test solutions, respectively. The energy barrier values against corrosion were also calculated in the presence and absence of inhibitor, with the help of surface coverage ratio and i_{corr} values for different temperatures.

Keywords Interfaces · Electrochemical techniques · Corrosion · Adsorption

G. Tansuğ (✉)
Ceyhan Engineering Faculty, Chemical Engineering Department, Cukurova University, 01950 Adana, Turkey
e-mail: gozde.tansug@gmail.com

T. Tüken · G. Sığırcık · G. Fındıkkıran · E. S. Giray · M. Erbil
, Sciences & Letters Faculty, Chemistry Department, Cukurova University, 01330 Adana, Turkey

Introduction

Specifically designed and synthesized green corrosion inhibitors have attracted much attention, since there is a necessity for development of environmentally friendly inhibitors [1–20]. The most important fields of inhibitor application are acid pickling, industrial acid cleaning, open water circulating systems, and heat exchangers [21–26]. There must be given much more attention for the systems employing different metals that galvanic couples are assembled [27–30]. For this reason, the organic molecules are tailored with specific functional groups like amine, thiol, and azole etc., for multitasking. The desired properties are high efficiency, low toxicity, and high stability in acidic environment, ease of synthesis, and cost efficiency. The inhibition efficiency of organic molecules is strongly related with the type and position of functional groups that govern the adsorptive interaction with metal surface. In some cases, the compatibility with corrosion products is also required, but this point is not necessarily considered for steel protection in acid solutions.

Even though there are many effective inhibitor molecules fashioned with various functional groups (amine, azole, carboxylate, mercapto, etc.), mercapto (i.e., thiol) functionalized molecules are generally the most efficient type for steel protection in acidic aqueous media [31–62]. The sulfur atom with unshared electrons can easily coordinate with vacant *d* orbitals of iron atoms aligned through the bare surface. The major role of azole and thiol groups is adsorptive interaction with the surface; the other sides of the molecule are designed to support adsorption. Simply, the negative charge density of functional group is responsible for the attraction and the rest of molecular design is to consolidate the strength of protective adsorption layer. Then, this organic layer is expected to play the role of a physical barrier between the metal and corrosive environment. The best auxiliary groups are those that can modify the solution side of the organic layer, in order to obtain less

hydrophobic and/or permeable nature [35, 51, 54, 63–65]. In the case where the auxiliary groups increase intermolecular attraction between the adsorbed molecules, a polymer-like layer could be obtained on the surface [66].

In the literature, it was reported that aminothiophenol (ATP) has inhibition efficiency at around 82 %, against steel corrosion in 1 M HCl solution [67]. In a recent publication, it was shown that the efficiency can much be enhanced with further modification of this molecule. It was reported that higher efficiency can be obtained by modifying this molecule, by help of simple reactions with acrylic acid and dodecylamine substances [68]. In another study, 77 % inhibition efficiency was reported for 2-ATP compound against steel corrosion in 0.1 M HCl test solution [69].

In this study, starting from 2-aminobenzenethiol and methylacetoacetate substances, we have synthesized methyl 3-((2-mercaptophenyl) imino) butanoate compound. Methylacetoacetate is also named as 3-oxobutanoic acid methyl ester; this substance is not considered within efficient corrosion inhibitors [70]. However, it gives reaction with 2-aminobenzenethiol to obtain derivatives functionalized with carboxylate tail which offers polarity and stronger attraction forces. The inhibition efficiency of this compound was studied against steel corrosion in 0.1 M HCl solution.

Experimental

Methyl 3-((2-mercaptophenyl) imino) butanoate (MMPB) was synthesized in our laboratory. For the synthesis of inhibitor compound, 2-aminobenzenethiol (1.25 g, 10 mmol), methylacetoacetate (1.26 g, 10 mmol), and 10 mol% of trifluoroacetic acid (TFA) were reacted in 5 ml ethanol, stirring in a round-bottomed flask. The temperature was set to 80 °C with the help of oil bath, during the reaction. Thin-layer chromatography (TLC) of the reaction mixture after 150 min showed the completion of the reaction. Then, the mixture reaction was filtered, and the solid product was washed with ethyl acetate. Then, the solvent residue was evaporated under reduced pressure to yield the crude product. Finally, the product was further purified via recrystallization from ethanol. The proceeded reaction was summarized in Fig. 1 [71].

The inhibition efficiency of the synthesized compound was studied in various concentrations of aqueous HCl solution, employing a three-electrode setup in one compartment cell.

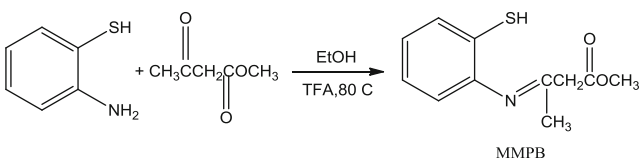

Fig. 1 The synthesis reaction of methyl 3-((2-mercaptophenyl) imino) butanoate (MMPB)

The reference electrode was Ag/AgCl (3 M KCl) and platinum wire as the counter electrode. The working electrode was steel (in wt%: 0.0820 C, 0.6210 Mn, 0.1810 Si, 0.0129 P, 0.0162 S, and balancing Fe), cylindrical rods are embedded in epoxy resin. The working surface area is 0.07 cm^2 for being subjected to corrosive test solution. Before each experiment, the specimens were mechanically abraded with silicon carbide papers (grades ranging from 500 to 1000), degreased with acetone, washed with distilled water, and dried. In order to determine corrosion rate, steel coupons (10×10×1 mm) were immersed in test solutions. These samples were treated with the same surface cleansing process, as described before.

The potentiodynamic (PD) and electrochemical impedance spectroscopy (EIS) measurements were carried out CHI 660C model electrochemical workstation. Prior to electrochemical measurements, the freshly cleaned electrodes were left in the test solution for 30 min until the steady state condition was reached. After this period, the measured open-circuit potential value is highly stable and considered as corrosion potential (E_{corr}). The initial value of PD measurements was this E_{corr} value and the scan rate was 1 mV s^{-1}, for all experiments. The EIS measurements were also performed using these E_{corr} values, employing 5 mV perturbation voltage and 10^{+4}–10^{-1} Hz frequency range.

For the assessment of inhibition mechanism, the effect of concentration and temperature variables were investigated. The studied temperature range was between 25 and 55 °C. Atomic absorption spectroscopy (AAS) was utilized for quantitative analysis of released iron ions, during the 18-h immersion tests. In order to investigate the morphology and structural composition of the surface, Zeiss/Supra 55 model field emission scanning electron microscope (FE-SEM).

Results and discussion

The effect of HCl concentration

The inhibition efficiency of synthesized inhibitor (MMPB) was firstly studied with the help of PD measurements in various concentrations (0.1, 0.5, and 1.0 M) of hydrochloric acid test solution (Fig. 2). For this purpose, 10 mM constant inhibitor concentration was employed. Before each measurement, the electrodes were left to reach steady-state conditions for 30 min. Then, the measured open-circuit potentials were handled as corrosion potential value (E_{corr}) and this value was employed as the initial point for PD measurement. The E_{corr} values were quite close to each other, for all concentrations of HCl. However, increasing HCl concentration increased the anodic dissolution rate regularly in inhibitor-free solutions. The concentrations of hydronium and chloride ions are crucial for dissolution rate of steel, since the surface conditions and anodic mechanism are governed by these ions [72]. In the case of inhibitor-added solutions, the reduction of anodic

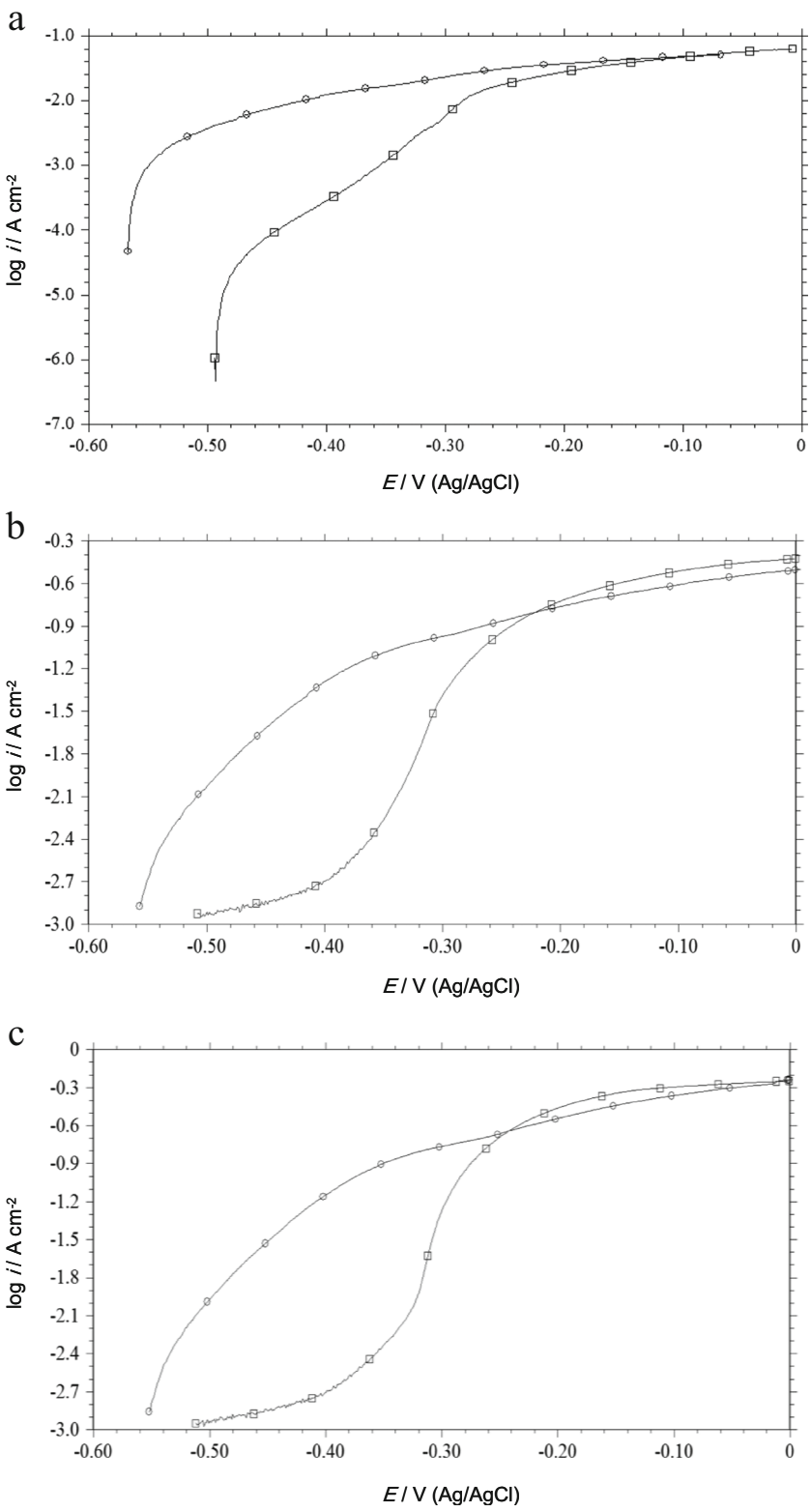

Fig. 2 Potentiodynamic measurement results in the absence (*empty circle*) and presence of 10 mM inhibitor (*empty square*) in various concentrations of HCl solutions at 25 °C; 0.1 M (**a**), 0.5 M (**b**), 1 M (**c**)

dissolution rate (i.e., measured anodic current density) was clearly seen for all HCl concentrations. Both chloride and hydronium concentration increases from dilute to concentrated HCl solutions, then the inhibitor exhibit lowers efficiency. The inhibition efficiency is related with the strength of adsorptive interaction between inhibitor and steel surface. Therefore, the highest inhibition efficiency was observed for 0.1 M HCl concentration. Generally, the efficiency is considerably high at potentials close to E_{corr} values. During the potential scan toward anodic domain, the inhibitor loses

efficiency, because the employed potential becomes dominant for anodic dissolution process at the interface. Owing to higher charge density, the adsorption of chloride ions becomes more favorable rather than the inhibitor, as the electrode potential becomes more and more positive.

The inhibition efficiency of MMPB was also studied with the help of EIS measurements, in different (0.1, 0.5, and 1.0 M) HCl solutions. The results were fitted with a simple R-CPE model and given in Fig. 3. The obtained fitting data are summarized in Table 1. In the case of inhibitor-free test solutions, the interfacial capacitance value (named $C_{M/S}$) increased gradually, as the HCl concentration increases. This case is related with the increasing hydronium and chloride ions concentration in solution, which influence the charge separation and surface excess along the metal/solution double layer. On the other hand, the $C_{M/S}$ values decreased with

Table 1 The solution resistance (R_s), polarization resistance (R_p), metal/solution interfacial capacitance ($C_{M/S}$) and inhibition efficiency (φ) for steel in the absence and presence of 10 mM MMPB, in different concentrations of HCl solution

HCl concentration (M)	R_p (Ω cm^2)		$C_{M/S}$ (μF cm^{-2})		φ
	Blank	Inhibitor	Blank	Inhibitor	
0.1	14	531	110	22	97.36
0.5	8	216	320	35	96.30
1.0	7.5	197	990	38	96.19

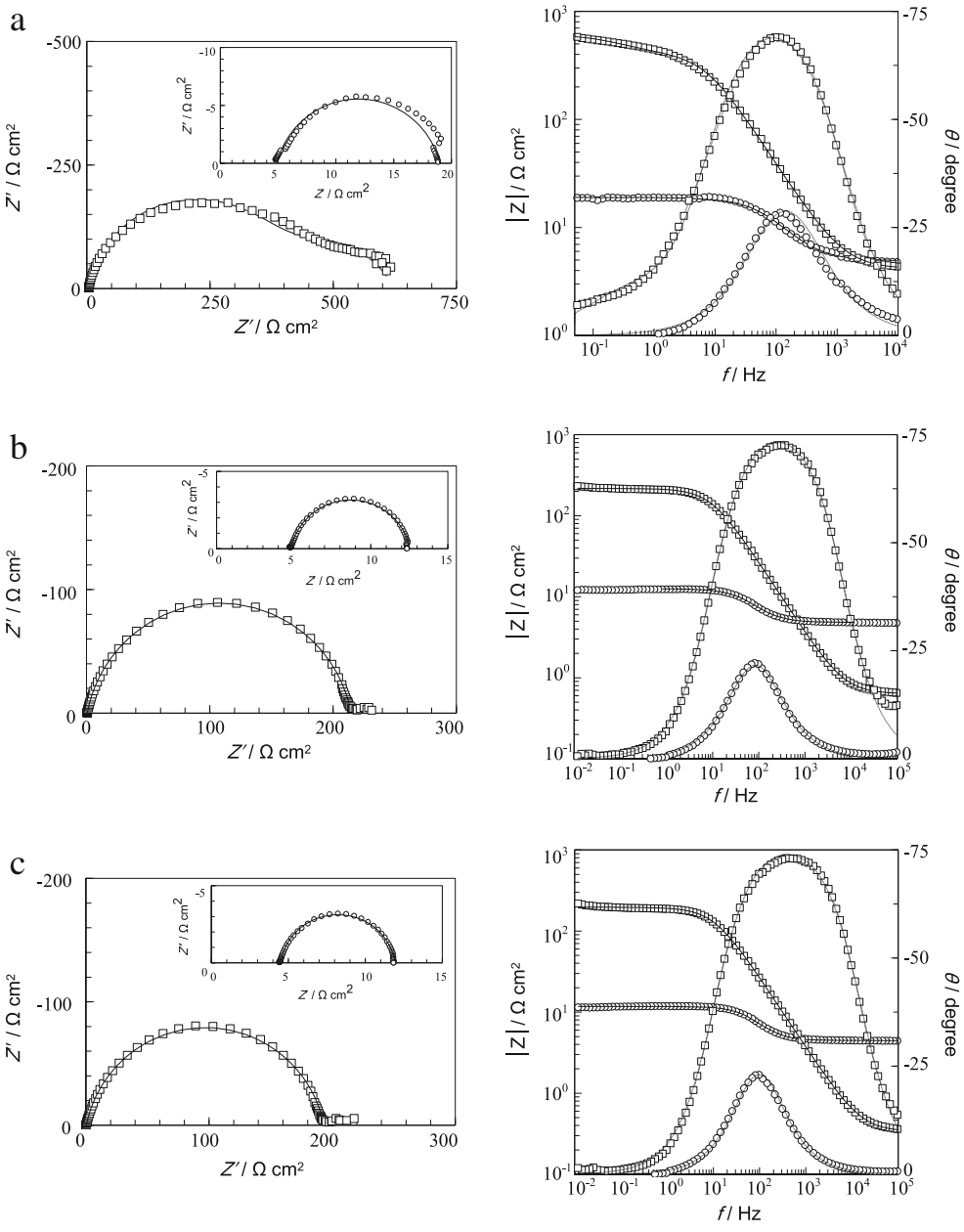

Fig. 3 The EIS results in the absence (*empty circle*) and presence of 10 mM inhibitor (*empty square*) in various concentrations of HCl solutions at 25 °C; 0.1 M (**a**), 0.5 M (**b**), 1 M (**c**) and fit results (*solid line*)

inhibitor addition, in all cases. This outcome is explained with strong adsorption of inhibitor molecules on the metal surface, and then the structure and dielectric properties of double layer changed. Also, the increase of R_p values was indicating to the protective adsorption layer on the surface. The said layer slowed down the attack of corrosive species and increased the R_p value. The variation of $C_{M/S}$ and R_p values are in strong correlation with the previously discussed PD results. The highest R_p and lowest $C_{M/S}$ values were measured in 10 mM inhibitor-containing 0.1 M HCl test solution.

The effect of inhibitor concentration

Essentially, the relation between the electrode surface potential and the strength of inhibitor adsorption is examined during PD measurements. As the potential value increased toward anodic domain (with respect to E_{corr}), the adsorptive interactions are governed by excess positive charge of electrode surface and relevant potential gradient through the solution side of interface. The inhibitor molecules and corrosive species are competitively adsorbed on the surface. The surface concentrations of these adsorbing species differ greatly, due to their charge densities and bulk concentrations. At this point, the chloride ion is highly advantageous against inhibitor molecule, with its smaller size and high charge density. In Fig. 4, the well-known activation-controlled anodic dissolution of steel is observed for inhibitor-free test solution. At potentials quite far from the E_{corr} value, mass transport limitations become predominant on dissolution rate, i.e., current density. In our case, these limitations are caused by desorption and removal of soluble corrosion products. In Fig. 4, it is clearly seen that the adsorption of inhibitor molecules is favored with increasing bulk concentration. Then, the corrosion potential (E_{corr}) value shifted to nobler values and anodic dissolution rate decreased significantly. As the metal/solution interface becomes electrified along the double layer, the metal side is induced by adsorbed ions and the surface

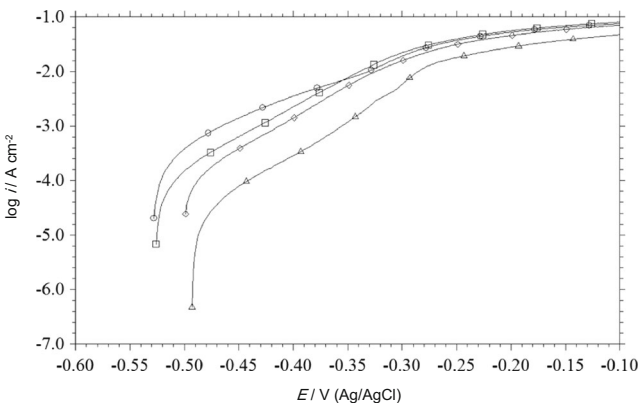

Fig. 4 Anodic polarization plots for steel after 60 min exposure time in 0.1 M HCl solutions, 0.5 mM (*empty circle*), 1 mM (*empty square*), 5 mM (*empty diamond*), and 10 mM (*empty upright triangle*) of MMPB solutions

becomes charged. The charge deposited along the double layer determines the quantitative value of double-layer capacitance and of course the electrode potential. Once the chloride ions are replaced with inhibitor molecules, the surface excess and charge deposition quantities will be totally different. The shift of corrosion potential is explained with the diversely structured double layer, as a result of strongly adhered inhibitor molecules on the metal surface [72].

The potential scan is continued toward more positive values, the anodic dissolution rates (current density) become very similar for all concentrations and inhibitor-free conditions. As the metal surface is polarized toward positive direction, the chloride ions get superiority against inhibitor molecules for competitive adsorption. Possessing high charge density, chloride ions will comprise most of the surface excess of negatively charged species. Moreover, the measured anodic current values were almost the same for all samples (Fig. 4), at potentials higher than −0.30 V (vs Ag/AgCl).

In Fig. 5, the EIS measurement results are given for blank test solution and various concentrations of inhibitor. In Bode diagrams, phase shift is clearly seen with the addition of 10 mM inhibitor; in the meantime, the R_p reached the value of 531 Ω cm^2. In log f–log Z plot, the linear region at high frequencies exhibits a slope slightly lower than −1, for all concentrations. Ideally, the slope would be −1 for a pure capacitor; this part is related with the capacitive behavior of interface. Then another linear region (where the slope is "zero") is observed at lower frequencies, at which the resistance behavior of interface becomes dominant. The intercept of these two linear regions named as breakpoint frequency and this value is characteristic for the interface. The shift of this value toward lower frequencies has meaning that the charge transfer is difficult at the interface. For a corroding metal, the retardation of charge transfer means that corrosion rate is reduced. The provided data indicated that corrosion process can be modeled by a simple circuit; constant phase element (CPE) and polarization resistance (R_p) were parallel connected, solution resistance (R_s) in series with them. The CPE was used for definition of capacitance and introduced for the description of frequency dependence. The admittance (Y_o) and exponential factor (n) characterize the phase shift of interfacial capacitance and surface conditions. From the perspective of dimension, CPE does not have the unit of capacitance (F cm^{-2} or Ω^{-1} cm^{-2} s); its dimension is given as Ω^{-1} cm^{-2} s^n. Mansfeld and Hsu developed an equation for unit correction and obtaining the accurate value of capacitance (Eq. (1)), when the data could be identified with simple R-CPE circuit [66, 73].

$$C_{CPC} = Y_0(2\pi f_{max})^{n-1} \quad (1)$$

The f_{max} value represents the frequency of the maximum on the $-Z''$. In this study, the capacitance value related to metal/solution interface ($C_{M/S}$) was calculated using fitting results.

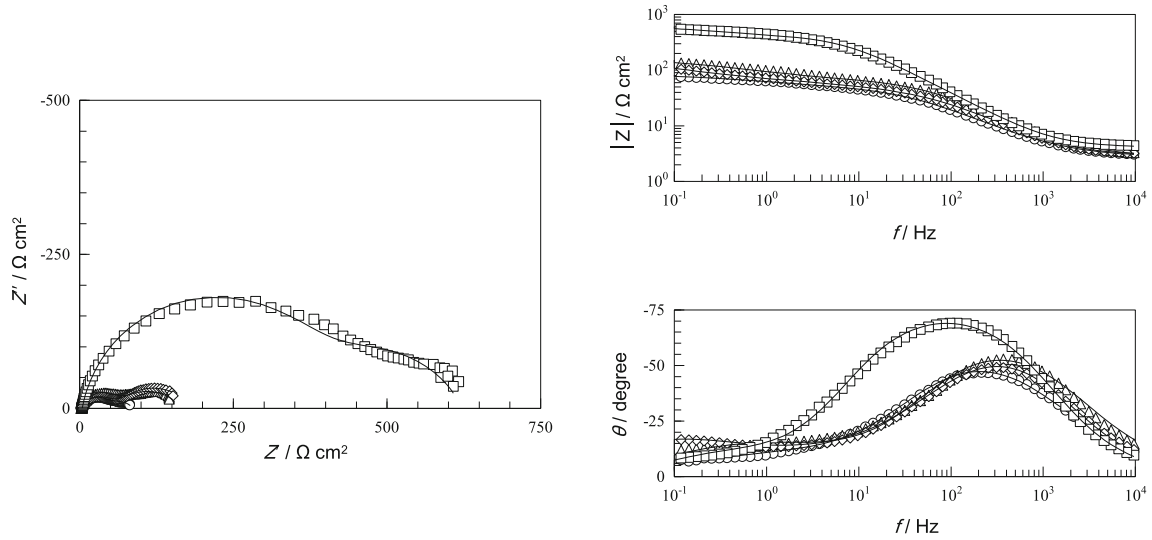

Fig. 5 The EIS results obtained in 0.1 M HCl solution at 25 °C, 0.5 mM (*empty circle*), 1 mM (*empty upright triangle*), 5 mM (*empty diamond*), 10 mM (*empty square*) MMPB concentrations and fit results (*solid line*)

$C_{M/S}$ values calculated using Eq. (1) and the inhibition efficiencies (φ) were calculated from polarization resistance values using Eq. (2), these values are summarized in Table 2.

$$\varphi = \frac{R_p - R_p^0}{R_p} \times 100 \quad (2)$$

In this equation R_p^0 and R_p represent the values measurement in the blank and inhibitor added solution, respectively.

In presence of 10 mM inhibitor, the $C_{M/S}$ value decreased down to 22.00 μF cm^{-2} (Table 1). The interfacial capacitance value is related with the surface coverage ratio that governed with inhibitor concentration. As a result of strong adsorptive interaction between the inhibitor molecules and metal surface, the water molecules and chloride ions are removed from the surface. Thus, the dielectric properties of electrical double-layer change remarkably. Also, the polarization resistance (R_p) value increased to 531 Ω cm^2, after 10 mM inhibitor addition. These results are compatible with the PD measurement results.

Moreover, the $C_{M/S}$ value decreased regularly with inhibitor concentration, as the R_p value increased. These results are consistent with physical barrier behavior of inhibitor molecules adsorbed on the metal surface. At higher bulk inhibitor concentrations, the surface concentration of inhibitor molecules increases, too. Then, the inhibitor adsorption becomes favorable and the surface coverage ratio (θ) increases.

Table 2 The polarization resistance (R_p), metal/solution interfacial capacitance ($C_{M/S}$) and inhibition efficiency (φ) for steel in 0.1 M HCl solution containing different concentrations of MMPB

C (mM)	R_p (Ω cm^2)	$C_{M/S}$ (μF cm^{-2})	φ
Blank	14	110.00	–
0.5	83	33.83	83.13
1	147	28.90	90.48
5	153	26.65	90.85
10	531	22.00	97.36

The adsorptive interaction with the surface is mainly attributed to the –SH group associated with the inhibitor molecule, while the intermolecular attraction along the carboxylate groups (at the other side of the molecule) provide molecular attractions between inhibitor molecules. The inhibition efficiency of adsorption layer is enhanced with the intermolecular forces developed between the carboxylate end groups of adsorbed inhibitor molecules.

Galvanic measurements were realized for better explanation of interaction between inhibitor and metal surface. For this purpose, identical steel electrodes were immersed in separate test solutions with and without inhibitor, and then coupled to each other. Galvanic current and potential difference was measured between these couples. For this purpose, two different flasks were filled up with inhibitor-free and 10 mM inhibitor-containing solutions, respectively. Then, a salt bridge was employed for ionic conductivity between half cells and the immersed coupon electrodes were connected to each other with external connection wires. The potential difference and passing current were measured against time between these two electrodes. A 50-mV potential difference was measured between coupled electrodes and net current flow was noted (Fig. 6). The setup worked like a galvanic cell between steel electrodes immersed in different solutions; with and without inhibitor. In one of the half-cells, the electrode potential was slightly nobler due to inhibitor adsorption on steel surface. As discussed before, the adsorption of inhibitor molecules changes the excess charge at the metal surface. Therefore, a potential difference develops between the electrodes immersed in blank and inhibitor-containing solutions,

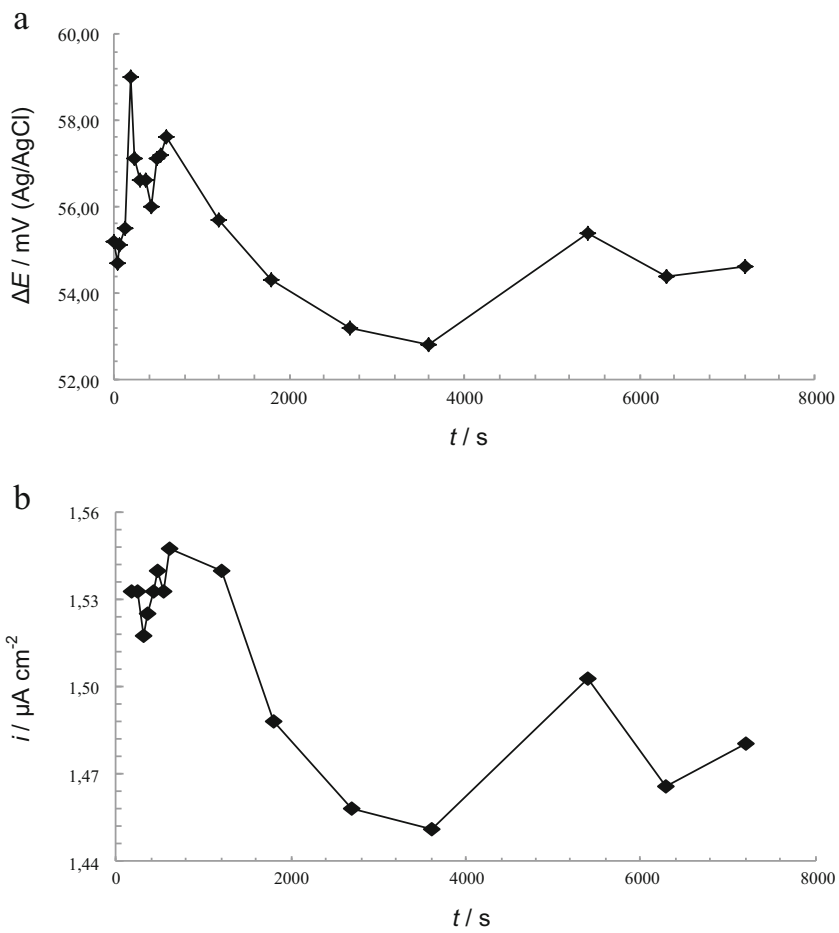

Fig. 6 Electrochemical potential difference (**a**) and current flow (**b**) between galvanically coupled steel samples immersed in 0.1 M HCl and 0.1 M HCl+10 mM MMPB solutions

respectively. The potential difference between two electrodes is the driving force for the current flow through the cell. According to this situation, the electrons are withdrawn by the electrode immersed in inhibitor-containing solution. The measured galvanic current density is about 1.5 μA. This value cannot be considered as corrosion current density, because the inhibitor does not offer prevention of anodic dissolution all over surface of the electrode immersed in inhibitor added test solution. Depending on the surface coverage ratio, the anodic dissolution process is partially blocked by inhibitor adsorption.

SEM measurements were realized for better understanding the effect of inhibitor on surface morphology, after exposure to corrosive environment. For this purpose, identical steel coupons were immersed in inhibitor-free and 10 mM inhibitor-containing test solutions, SEM micrographs were taken after 4 days exposure period and given in Fig. 7. In inhibitor-free solution, the surface was highly damaged due to severe corrosion. The effect of chloride ions on the kinetics and mechanism of iron dissolution has long been studied extensively in the literature [74–76]. For the same reason, the corrosion process takes place all over the surface. However, it is apparent that some regions are abraded at a higher ratio, due to some microstructural differences from side to side of the steel sample. Moreover, the surface was highly rough, at the end of immersion test in blank solution. In Fig. 7b, it is seen that the surface remained highly smooth and there was no evidence for severe corrosion. There was not any evidence for polymer-like film formation or protective stable compound on the surface, the little gatherings appeared on the surface were considered as nonprotective residue from testing solution.

Effect of temperature

The temperature effect was investigated to understand the inhibitor mechanism by using PD and EIS measurements. The PD results are given for inhibitor-free and 10 mM MMPB concentration in a temperature range between 25 and 55 °C. As seen from Fig. 8, the anodic current densities increase remarkably for both conditions; in the absence and presence of inhibitor, with temperature. In other words, the anodic dissolution rate increases in both cases, as the temperature is elevated. It can be seen that the inhibitor addition reduced the anodic dissolution rate for all temperatures, comparing the plots given for the absence (Fig. 8a) and presence (Fig. 8b) of inhibitor for a given temperature. The inhibitor adsorption and surface

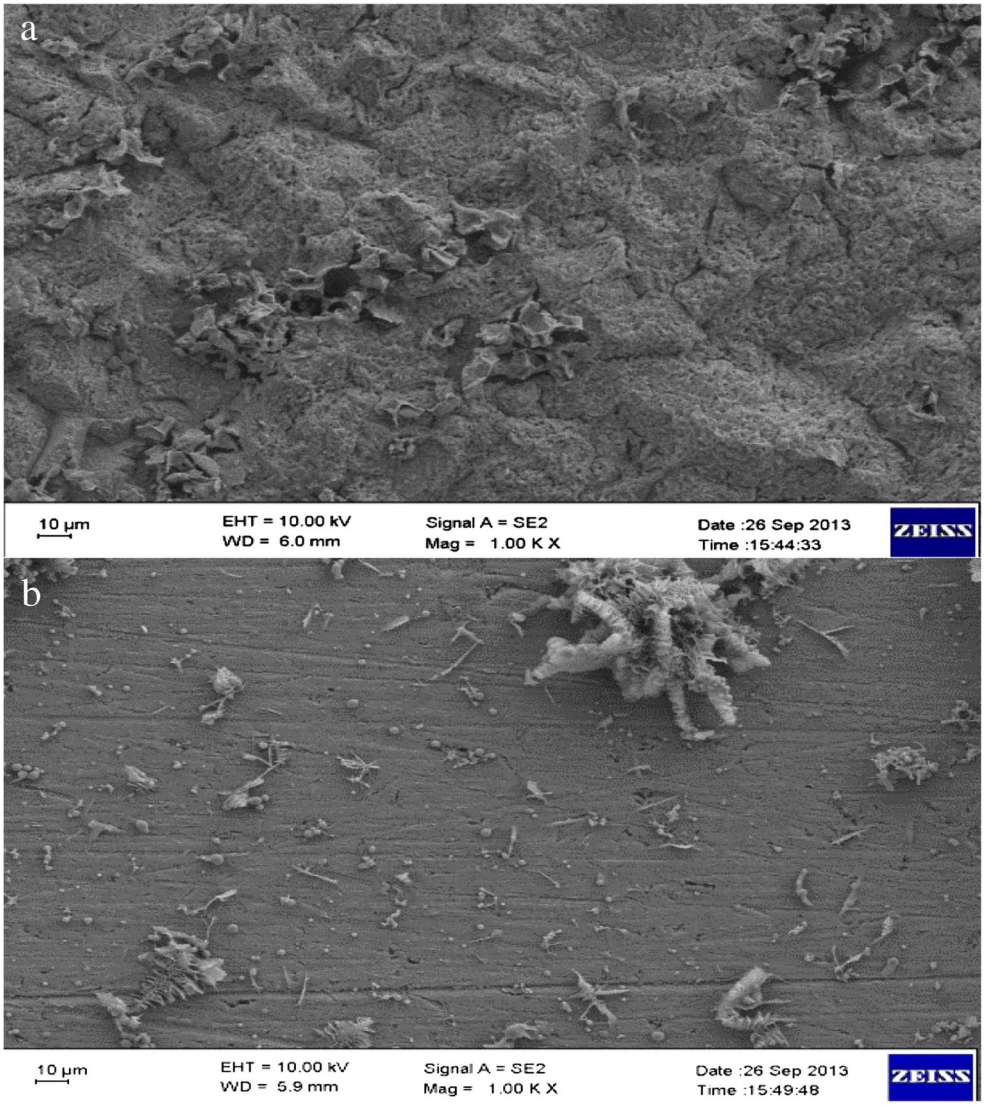

Fig. 7 SEM images of steel coupons after 4 days exposure to 0.1 M HCl (**a**) and 0.1 M HCl+ 10 mM MMPB (**b**)

coverage ratio are sensible against temperature change. Desorption of weakly adsorbed species is favored by temperature increase and it becomes easier to overcome the energy barrier against charge transfer. For the same reason, E_{corr} values shifted to negative direction for all testing solutions, either with or without inhibitor.

In Figs. 9 and 10, the EIS results are given for various temperature conditions. From this data, the capacitance and polarization resistance values were determined and summarized in Table 2. In 10 mM MMPB-containing solution, the R_p value decreased from 531 to 82 Ω cm^2 as the temperature goes from 25 to 55 °C. For the same temperature range, the $C_{M/S}$ values decreased from 22.00 to 4.36 μF cm^{-2}. This situation is related with weak adsorptive interaction between the inhibitor molecules and steel surface, under elevated temperatures. As can be seen, the $C_{M/S}$ value decreased gradually with temperature, in inhibitor-free solution too. In all cases, the surface excess of adsorbing species (either organics or ions) reduces with increasing temperature. Then, the capacitance value corresponding to metal/solution interface differs significantly. However, the calculated inhibition efficiency (φ) remained reasonably high until 45 °C, but this value was 91 % for 55 °C temperature condition (Table 3).

During temperature studies, the corrosion rate increases for both blank and inhibitor-added test solution. Then, the relative inhibition efficiency observed from electrochemical techniques may not change significantly. However, the real quantity of i_{corr} is the direct measure for deterioration rate of metal, under elevated temperatures. Because the calculated efficiency may sound sufficient but the corrosion loss may not be tolerable at elevated temperatures. For this reason, atomic adsorption spectroscopy (AAS) was used to determine the quantity of iron ions released to the testing solution during the steel corrosion for 18 h immersion period. The experiments were realized for the whole set of the temperature range, from 25 to

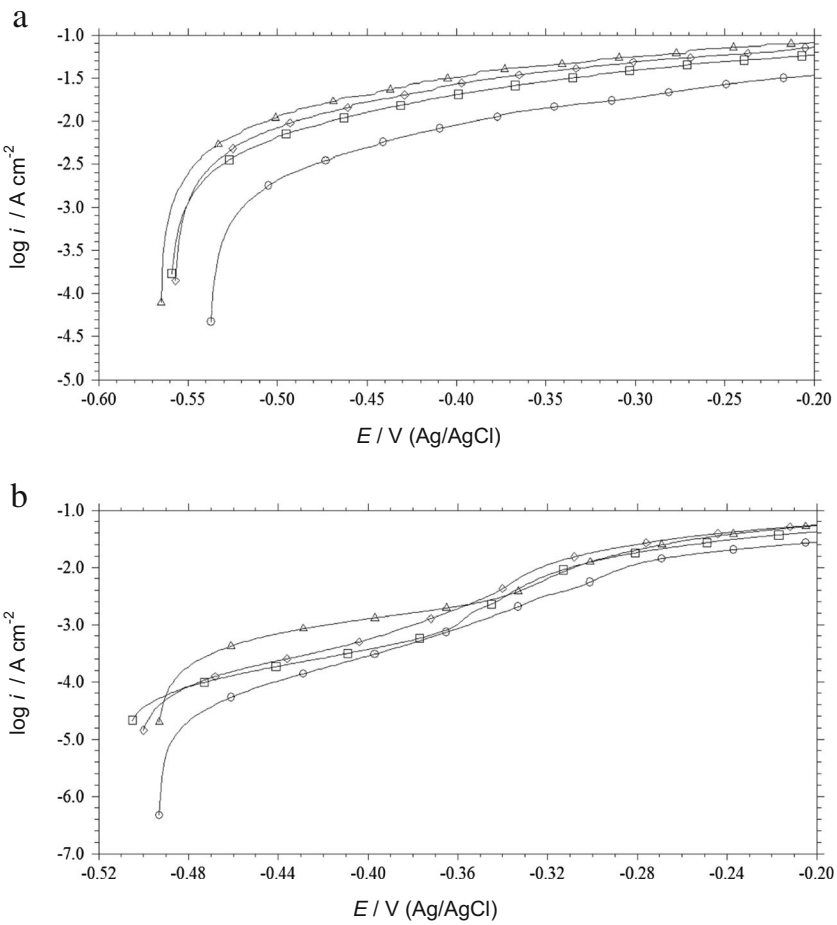

Fig. 8 Anodic polarization plots for steel after 60 min exposure time in 0.1 M HCl (**a**) and 0.1 M HCl+10 mM MMPB (**b**) solutions; 25 °C (*empty circle*), 35 °C (*empty square*), 45 °C (*empty diamond*), 55 °C (*empty upright triangle*)

55 °C. Based on the Faraday's law, the corrosion current (i_{corr}) values were calculated using the amount of iron content in test solution. By doing so, the obtained i_{corr} values are the mean values representing the whole immersion period. The surface

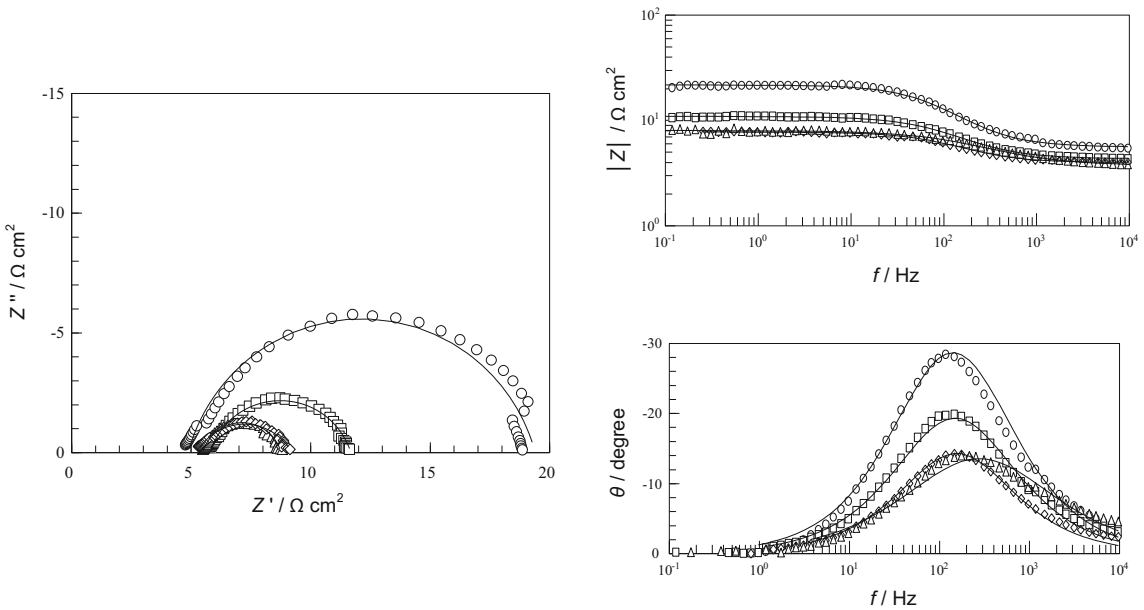

Fig. 9 The EIS results for steel after 30 min exposure time in 0.1 M HCl inhibitor-free solution at 25 °C (*empty circle*), 35 °C (*empty square*), 45 °C (*empty upright triangle*), 55 °C (*empty diamond*), and fit results (*solid line*)

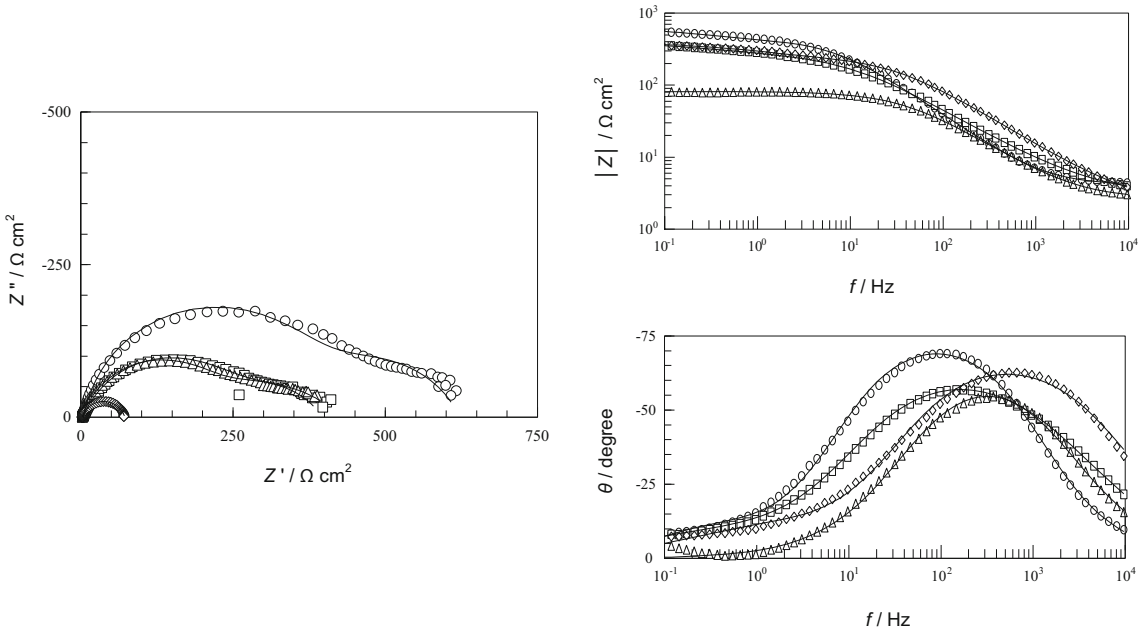

Fig. 10 The EIS results for steel after 30 min exposure time in 0.1 M HCl +10 mM MMPB solution at 25 °C (*empty circle*), 35 °C (*empty square*), 45 °C (*empty upright triangle*), 55 °C (*empty diamond*), and fit results (*solid line*)

coverage ratio (θ) values are also calculated with using these i_{corr} values (Eq. (3)) and all these results are given in Table 4.

$$\theta = 1 - \frac{i}{i_o} \tag{3}$$

In this equation, i_o and i represent the values measured in the blank and inhibitor added solutions, respectively.

The value of θ gives idea about the strength of adsorptive interaction between the surface and inhibitor molecules, under elevated temperatures. Moreover, the i_{corr} value was 75 μA cm^{-2} and inhibition efficiency value was 96 %, under 55 °C.

In order to discuss the inhibition mechanism, the activation energy (E_a) values were determined with help of Arrhenius equation. For this purpose, the i_{corr} and θ values obtained from AAS measurements were utilized. From its definition, the value of E_a is directly related to the reaction steps and overall mechanism. In corrosion process, the discussed E_a value includes the chemical and electrical energy involved for the electrochemical reaction. In acidic chloride solutions, the corrosion mechanism is generally given with a few steps including halide ion adsorption [74–76]. In Fig. 11a, the experimental data is given as a graph, at which the ln i_{corr} values are plotted against 1/T. Generally, the E_a values are calculated from the slope of these plots and handled as energy barrier value against the iron dissolution due to corrosion. By doing so, 14.17 kcal mol^{-1} of E_a value was obtained for inhibitor-free solution.

According to the definition of Arrhenius equation, the E_a value could only change when the reacting species or mechanism changes. With its thiol and azole functional groups, the inhibitor molecule could strongly adsorb on the steel surface. The covered surface area is protected against corrosive attack, while the rest of surface (not covered with adsorbed inhibitor) is still subjected to corrosion. In the case of inhibitor solution, the i_{corr} values are given for the entire surface but the anodic

Table 3 The polarization resistance (R_p), metal/solution interfacial capacitance ($C_{M/S}$) values of steel in absence of inhibitor and presence of 10 mM inhibitor solutions, inhibition efficiency (φ) for different temperatures

T (°C)	R_p (Ω cm^2)		$C_{M/S}$ (μF cm^{-2})		φ
	Blank	Inhibitor	Blank	Inhibitor	
25	14	531	110.00	22.00	97.36
35	10	422	41.03	10.46	97.63
45	7	390	27.90	7.59	98.20
55	7	82	15.76	4.36	91.50

Table 4 The corrosion current (i_{corr}) and surface coverage ratio (θ) values determined from evaluation of AAS results, for inhibitor-free and 10 mM inhibitor-containing solutions

T (°C)	$C_{Fe^{+2}}$ (mg L^{-1})		i_{corr} (μA cm^{-2})		θ
	Blank	Inhibitor	Blank	Inhibitor	
25	152.0	15.48	200.30	20.40	0.90
35	417.3	23.03	550.00	30.40	0.94
45	758.8	36.57	1000.00	48.20	0.95
55	1472.0	56.89	1940.00	75.00	0.96

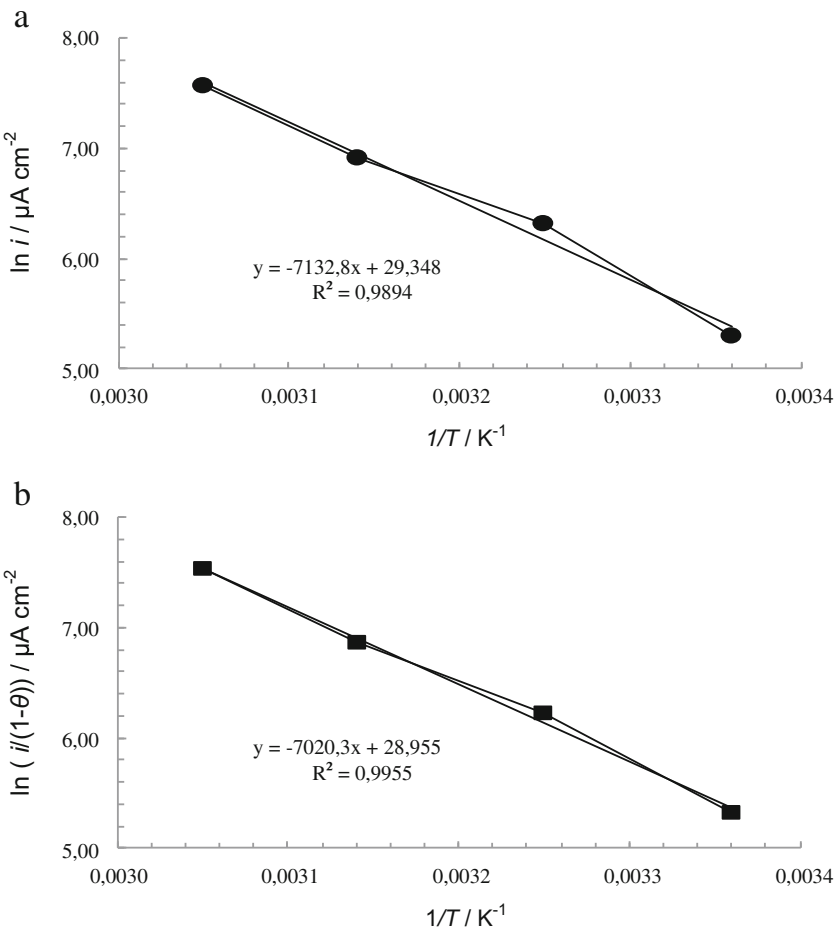

Fig. 11 Determination of activation energy values (E_a), T^{-1} versus ln i for inhibitor-free (**a**) and T^{-1} versus ln (i/(1−θ)) (**b**)

dissolution could take place only at instantaneously open surface regions. The corrosion mechanism at these points must be the same with inhibitor-free conditions. The azole compounds are known to form stable complex structures with copper ions. If the freshly released iron ions were to react with inhibitor molecules to give such complexes, then the dissolution mechanism may be altered. However, there is no clue for such products formation between Fe (II, III) and inhibitor, from interpretation of electrochemical and SEM results.

Therefore, the i_{corr} values obtained from AAS studies must be handled carefully, taking into account that the surface is covered to some degree. Then, the calculated i_{corr} value should be related to surface coverage ratio and should be given with the following equations [72].

$$i = k(1-\theta) \tag{4}$$

$$i = (1-\theta)Ae^{-E_a/RT} \tag{5}$$

The effect of surface coverage ratio is taken into account with the following equation, for evaluation of the relation between the current and temperature. For each temperature, the θ values and i_{corr} values were determined from AAS results and first term of Eq. (6) was plotted against 1/T.

$$ln\left(\frac{i}{1-\theta}\right) = \ln A - \frac{E_a}{RT} \tag{6}$$

After the correction brought to the rate term in this equation, the E_a value was determined from the slope of plot given in Fig. 11b, for 10 mM inhibitor concentration it is 58.37 kJ mol^{-1}. It must be noted that the E_a value was almost the same in the absence and presence of inhibitor. This shows

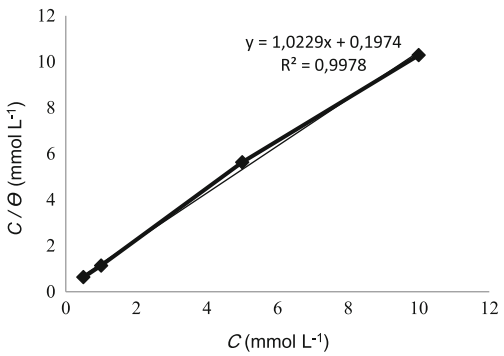

Fig. 12 Langmuir adsorption isotherm for adsorption of MMPB on steel

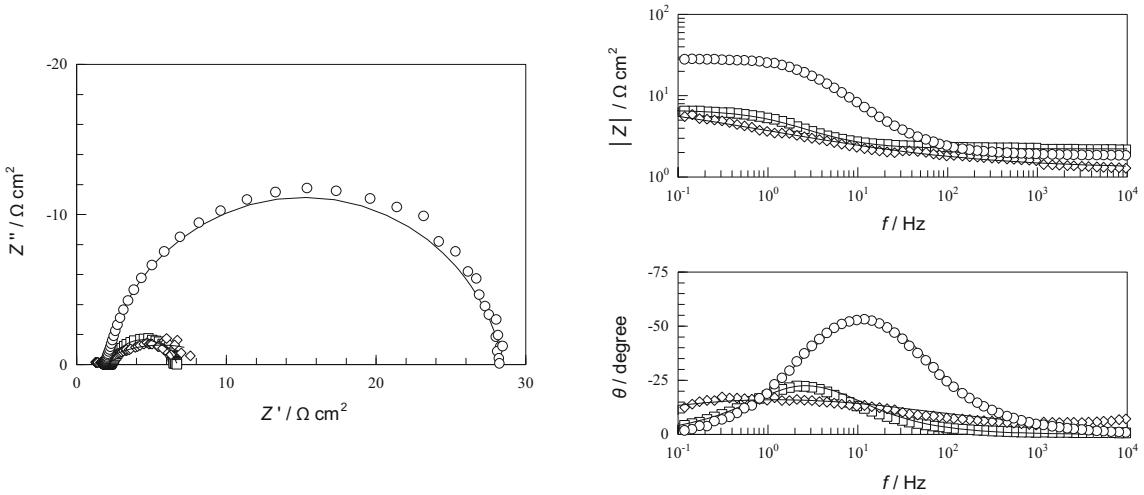

Fig. 13 The EIS results in 0.1 M HCl solution at 25 °C for different immersion time; 24 h (*empty circle*), 96 h (*empty square*), 192 h (*empty diamond*), and fit results (*solid line*)

that the inhibitor does not have a spectacular impact on the corrosion mechanism of steel in HCl environment, its efficiency is directly related to surface coverage ratio. In this context, it can be concluded that inhibition efficiency is a result of physical adsorptive interaction. Once the surface is blocked by inhibitor molecules, the attack of corrosive environment is hindered to some degree.

For further discussion of inhibitor adsorption mechanism, the isotherm was plotted and given in Fig. 12. Langmuir isotherm is based on the assumptions that the adsorption is provided by physical attractions and this event is reversible, therefore equilibrium could be defined between the rates of adsorption and desorption [66]. Relating the adsorption and desorption rates with surface coverage ratio gives the following Eq. 7.

$$\frac{C_{\text{inh}}}{\theta} = \frac{1}{K_{\text{ads}}} + C_{\text{inh}} \tag{7}$$

Where 55.5 is the molar concentration of water, R is the universal gas constant, and T is the temperature.

$$K_{\text{ads}} = \frac{1}{55.5} e^{-\frac{\Delta G^{\circ}_{\text{ads}}}{RT}} \tag{8}$$

From the intercept of the plot, the K_{ads} value was 5065.90, from Eq. 8 the adsorption free energy ($\Delta G^{\circ}_{\text{ads}}$) value was found −31.09 kJ mol^{-1}. These values support the idea that there is strong adsorptive interaction between the inhibitor and steel surface under the studied conditions [5, 36, 72]. The experimental data was quite well in agreement with the Langmuir isotherm and good correlation was notified. The results corroborated the previous discussions that the inhibitor molecules strongly adsorb on the surface, via physical attractions. The functional groups of synthesized inhibitor molecule are responsible for this attraction. At the interface, the adsorbed

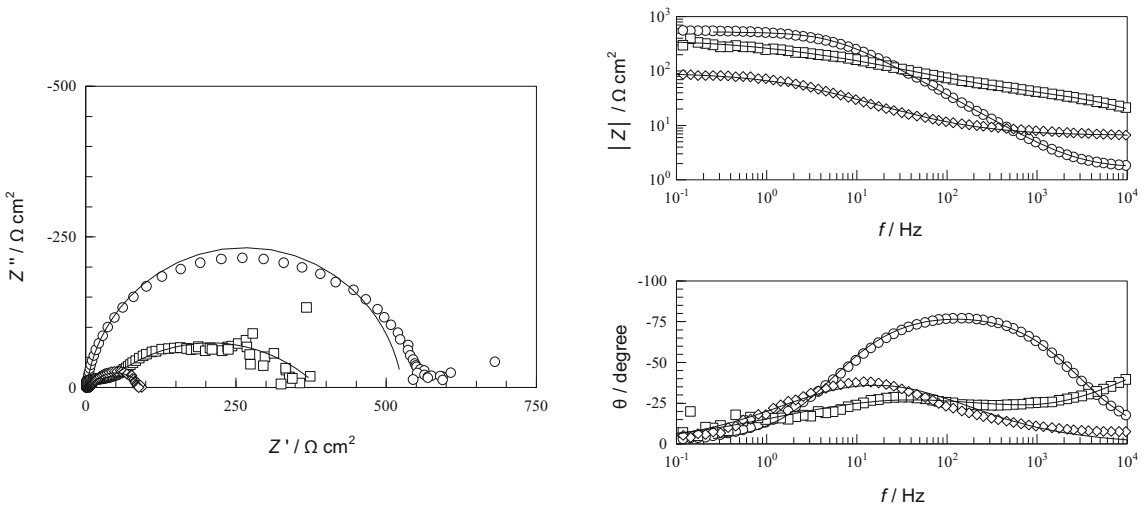

Fig. 14 The EIS results in 0.1 M HCl +10 mM MMPB solution at 25 °C for different immersion time; 24 h (*empty circle*), 96 h (*empty square*), 192 h (*empty diamond*), and fit results (*solid line*)

inhibitor molecules reduce the metal surface area that is vulnerable against the attack of corrosive species (Cl^-, H^+, etc.).

In the literature, 97.9 and 97.2 % inhibition efficiencies were reported for 10 mM 2,5-bis (4-dimethylaminophenyl)-1,3,4-thiadiazole and 2,5-bis (4-dimethylaminophenyl)-1,3,4-oxadiazole in 1 M HCl acid solutions [46]. Also, lower efficiency values were reported for 20 mM 2,5-bis(2-pyridyl)-1,3,4-thiadiazole [45] and 20 mM 2,5-bis(3-pyridyl)-1,3,4-thiadiazole [41] in 1 M HCl solutions as 84.4 and 94.5 %, respectively. On the other hand, Popova et al. investigated inhibition efficiencies for 10 mM 1-H benzotriazole (BTA) and 1,3-benzothiazole (BNS) in 1 M HCl solutions, respectively, 84 and 81 % efficiencies were reported [61]. Considering similar inhibitors reported recently, the synthesized MMPB has good inhibition efficiency and its molecular design offers good stability, too.

The efficiency of inhibitor was also tested against immersion time; for this purpose, steel electrode was immersed in blank and 10 mM inhibitor-containing test solutions and EIS measurements were realized periodically. In Figs. 13 and 14, some typical EIS results are selected and given for 24, 96, and 192 h exposure periods. In both test solutions, the R_p value decreased significantly with time. In all cases, the R_p values were higher in inhibitor-added solution, with respect to blank test solution.

Generally, the corrosion rate increases with immersion time, if there is no possibility for the formation of protective layer or passive film consisting of insoluble iron products. Because, the surface conditions change significantly thanks to deterioration and presence of corrosion products at the interface. The adsorption strength of inhibitor decreased with time for the same reason. As a result, the R_p value decreased. From evaluation of R_p values (Eq. 2), the percent inhibition efficiencies were calculated and it was shown that MMPB exhibits notably high efficiency after extended immersion periods. The efficiency value was calculated to be 95 % after 24 h; this value became 93 % after 192 h immersion period. It was believed that the intermolecular attraction forces between carboxylate tails groups are helpful for consolidation of stable inhibitor adsorption layer on the surface.

Conclusion

Methyl 3-((2-mercaptophenyl) imino) butanoate (MMPB) compound was synthesized and investigated as corrosion inhibitor for steel. The efficiency was tested for various HCl concentrations (0.1, 0.5, and 1.0 M) and it was shown that the efficiency is higher than 95 %, for all cases. PD and EIS study results showed that inhibition efficiency of MMPB is a result of strong adsorptive interaction with steel surface. The studies subjecting the effect of inhibitor concentration revealed that 5 mM is the minimal dosage required for efficiencies higher than 90 %; moreover, 97.36 % efficiency is obtained with 10 mM MMPB concentration. From solution assay analysis, the i_{corr} value was found as 20.40 and 200.30 μA cm^{-2}, in 10 mM inhibitor and blank test solutions, respectively. These results were also used for determination of surface coverage ratio (θ) values. The value of energy barrier (E_a) against steel corrosion was calculated for blank and 10 mM inhibitor-containing test solutions. The effect of θ value was taken into account for employment of the Arrhenius equation, the corrosion rates were normalized with respect to surface coverage ratio in inhibitor-containing solutions. It was proved that the E_a value is almost the same for both conditions (in the absence and presence of inhibitor), thus the corrosion mechanism is said not to change with inhibitor addition. Strongly adsorbed inhibitor molecules cover the surface and hinder the corrosive attack. It was also shown that good efficiency values could be obtained even after extended immersion periods, 93 % after 192 h.

References

1. Torres VV, Rayol VA, Magalhães M et al (2014) Study of thioureas derivatives synthesized from a green route as corrosion inhibitors for mild steel in HCl solution. Corros Sci 79:108–118
2. Obot IB, Ebenso EE, Kabanda MM (2013) Metronidazole as environmentally safe corrosion inhibitor for mild steel in 0.5 M HCl: Experimental and theoretical investigation. J Environ Chem Eng 1: 431–439
3. Raja PB, Sethuraman MG (2008) Natural products as corrosion inhibitor for metals in corrosive media—a review. Mater Lett 62: 113–116
4. Negm NA, Kandile NG, Aiad IA et al (2011) New eco-friendly cationic surfactants: synthesis, characterization and applicability as corrosion inhibitors for carbon steel in 1 N HCl. Colloids Surf A 391: 224–233
5. Moretti G, Guidi F, Grion G (2004) Tryptamine as a green iron corrosion inhibitor in 0.5 M deaerated sulphuric acid. Corros Sci 46:387–403
6. Ghareba S, Omanovic S (2010) Interaction of 12-aminododecanoic acid with a carbon steel surface: towards the development of 'green' corrosion inhibitors. Corros Sci 52:2104–2113
7. Deng Q, Ding NN, Wei XL et al (2012) Identification of diverse 1,2, 3-triazole-connected benzyl glycoside-serine/threonine conjugates as potent corrosion inhibitors for mild steel in HCl. Corros Sci 64:64–73
8. Fragoza-Mar L, Olivares-Xometl O, Domínguez-Aguilar MA et al (2012) Corrosion inhibitor activity of 1,3-diketone malonates for mild steel in aqueous hydrochloric acid solution. Corros Sci 61: 171–184
9. Flores EA, Olivares O, Likhanova NV et al (2011) Sodium phthalamates as corrosion inhibitors for carbon steel in aqueous hydrochloric acid solution. Corros Sci 53:3899–3913
10. Zhang F, Tang Y, Cao Z et al (2012) Performance and theoretical study on corrosion inhibition of 2-(4-pyridyl)-benzimidazole for mild steel in hydrochloric acid. Corros Sci 61:1–9
11. Tao Z, Zhang S, Li W et al (2009) Corrosion inhibition of mild steel in acidic solution by some oxo-triazole derivatives. Corros Sci 51: 2588–2595

12. Karthikaiselvi R, Subhashini S (2012) The water soluble composite poly (vinylpyrrolidone–methylaniline): A new class of corrosion inhibitors of mild steel in hydrochloric acid media. Arab. J. Chem. In Press
13. Yadav M, Behera D, Sharma U (2012) Nontoxic corrosion inhibitors for N80 steel in hydrochloric acid. Arab. J. Chem. In Press
14. Zhang S, Tao Z, Liao S et al (2010) Substitutional adsorption isotherms and corrosion inhibitive properties of some oxadiazol-triazole derivative in acidic solution. Corros Sci 52:3126–3132
15. Ita BI, Offiong OE (2001) The study of the inhibitory properties of benzoin, benzil, benzoin-(4-phenylthiosemicarbazone) and benzil-(4-phenylthiosemicarbazone) on the corrosion of mild steel in hydrochloric acid. Mater Chem Phys 70:330–335
16. Singh AK, Shukla SK, Singh M et al (2011) Inhibitive effect of ceftazidime on corrosion of mild steel in hydrochloric acid solution. Mater Chem Phys 129:68–76
17. Deng Q, Shi HW, Ding NN et al (2012) Novel triazolyl bis-amino acid derivatives readily synthesized via click chemistry as potential corrosion inhibitors for mild steel in HCl. Corros Sci 57:220–227
18. Migahed MA, Abdul-Raheim AM, Atta AM et al (2010) Synthesis and evaluation of a new water soluble corrosion inhibitor from recycled poly (ethylene terephthalate). Mater Chem Phys 121:208–214
19. Deng Q, He XP, Shi HW et al (2012) Concise Cu^{1}-catalyzed azide-alkyne 1,3-dipolar cycloaddition reaction ligation remarkably enhances the corrosion inhibitive potency of natural amino acids for mild steel in HCl. Ind Eng Chem Res 51:7160–7169
20. Cai L, Fu Q, Shi R et al (2014) Pungent copper surface resists acid corrosion in strong HCl solutions. Ind Eng Chem Res 53:64–69
21. Zaferani SH, Sharifi M, Zaarei D et al (2013) Application of eco-friendly products as corrosion inhibitors for metals in acid pickling processes—a review. J Environ Chem Eng 1:652–657
22. Mahgoub FM, Abdel-Nabey BA, El-Samadisy YA (2010) Adopting a multipurpose inhibitor to control corrosion of ferrous alloys in cooling water systems. Mater Chem Phys 120:104–108
23. Liu F, Lu X, Yang W et al (2013) Optimizations of inhibitors compounding and applied conditions in simulated circulating cooling water system. Desalination 313:18–27
24. Azghandi MV, Davoodi A, Farzi GA et al (2012) Water-base acrylic terpolymer as a corrosion inhibitor for SAE1018 in simulated sour petroleum solution in stagnant and hydrodynamic conditions. Corros Sci 64:44–54
25. Abd-El-Khalek DE, Abd-El-Nabey BA (2013) Evaluation of sodium hexametaphosphate as scale and corrosion inhibitor in cooling water using electrochemical techniques. Desalination 311:227–233
26. Dkhireche N, Dahami A, Rochdi A et al (2013) Corrosion and scale inhibition of low carbon steel in cooling water system by 2-propargyl-5-*o*-hydroxyphenyltetrazole. J Ind Eng Chem 19:1996–2003
27. Wilhelm EJ, Ereneta VG (1973) Corrosion inhibitor control in aqueous solutions evaluated with galvanic couples. Corros Sci 13:1003–1017
28. Izquierdo J, Nagy L, Santana JJ et al (2011) A novel microelectrochemical strategy for the study of corrosion inhibitors employing the scanning vibrating electrode technique and dual potentiometric/amperometric operation in scanning electrochemical microscopy: application to the study of the cathodic inhibition by benzotriazole of the galvanic corrosion of copper coupled to iron. Electrochim Acta 58:707–716
29. Ai JZ, Guo XP, Chen ZY (2006) The adsorption behavior and corrosion inhibition mechanism of anionic inhibitor on galvanic electrode in 1 % NaCl solution. Appl Surf Sci 253:683–688
30. Kallip S, Bastos AC, Yasakau KA et al (2012) Synergistic corrosion inhibition on galvanically coupled metallic materials. Electrochem Commun 20:101–104
31. Moretti G, Guidi F, Fabris F (2013) Corrosion inhibition of the mild steel in 0.5 M HCl by 2-butyl-hexahydropyrrolo [1,2-b] [1,2] oxazole. Corros Sci 76:206–218
32. Fouda AS, Ellithy AS (2009) Inhibition effect of 4-phenylthiazole derivatives on corrosion of 304L stainless steel in HCl solution. Corros Sci 51:868–875
33. Musa AY, Kadhum AAH, Mohamad AB et al (2010) On the inhibition of mild steel corrosion by 4-amino-5-phenyl-4*H*-1,2,4-trizole-3-thiol. Corros Sci 52:526–533
34. Wang HL, Liu RB, Xin J (2004) Inhibiting effects of some mercapto-triazole derivatives on the corrosion of mild steel in 1.0 M HCl medium. Corros Sci 46:2455–2466
35. Cheng XL, Ma HY, Chen SH et al (1998) Corrosion of stainless steels in acid solutions with organic sulfur-containing compounds. Corros Sci 41:321–333
36. Popova A, Sokolova E, Raicheva S et al (2003) AC and DC study of the temperature effect on mild steel corrosion in acid media in the presence of benzimidazole derivatives. Corros Sci 45:33–58
37. Wang HL, Fan HB, Zheng JS (2003) Corrosion inhibition of mild steel in hydrochloric acid solution by a mercapto-triazole compound. Mater Chem Phys 77:655–661
38. Mahdavian M, Ashhari S (2010) Corrosion inhibition performance of 2-mercaptobenzimidazole and 2-mercaptobenzoxazole compounds for protection of mild steel in hydrochloric acid solution. Electrochim Acta 55:1720–1724
39. Álvarez-Bustamante R, Negrón-Silva G, Abreu-Quijano M et al (2009) Electrochemical study of 2-mercaptoimidazole as a novel corrosion inhibitor for steels. Electrochim Acta 54:5393–5399
40. Sherif EM (2014) Corrosion inhibition in 2.0 M sulfuric acid solutions of high strength maraging steel by aminophenyl tetrazole as a corrosion inhibitor. Appl Surf Sci 292:190–196
41. Bentiss F, Lebrini M, Vezin H et al (2004) Experimental and theoretical study of 3-pyridyl-substituted 1,2,4-thiadiazole and 1,3,4-thiadiazole as corrosion inhibitors of mild steel in acidic media. Mater Chem Phys 87:18–23
42. Bentiss F, Lebrini M, Lagrenée M (2005) Thermodynamic characterization of metal dissolution and inhibitor adsorption processes in mild steel/2,5-bis (*n*-thienyl)-1,3,4-thiadiazoles/hydrochloric acid system. Corros Sci 47:2915–2931
43. Elkadi L, Mernari B, Traisnel M et al (2000) The inhibition action of 3,6-bis (2-methoxyphenyl)-1,2-dihydro-1,2,4,5-tetrazine on the corrosion of mild steel in acidic media. Corros Sci 42:703–719
44. Bentiss F, Traisnel M, Lagrenee M (2000) The substituted 1,3,4-oxadiazoles: a new class of corrosion inhibitors of mild steel in acidic media. Corros Sci 42:127–146
45. El Azhar M, Mernari B, Traisnel M et al (2001) Corrosion inhibition of mild steel by the new class of inhibitors [2,5-bis (*n*-pyridyl)-1,3,4-thiadiazoles] in acidic media. Corros Sci 43:2229–2238
46. Bentiss F, Traisnel M, Vezin H et al (2004) 2,5-Bis (4-dimethylaminophenyl)-1,3,4-oxadiazole and 2,5-bis (4-dimethylaminophenyl)-1,3,4-thiadiazole as corrosion inhibitors for mild steel in acidic media. Corros Sci 46:2781–2792
47. Al-Sarawy AA, Fouda AS, Shehab El-Dein WA (2008) Some thiazole derivatives as corrosion inhibitors for carbon steel in acidic medium. Desalination 229:279–293
48. Ali SA, Saeed MT, Rahman SU (2003) The isoxazolidines: a new class of corrosion inhibitors of mild steel in acidic medium. Corros Sci 45:253–266
49. Tao Z, Zhang S, Li W et al (2009) Corrosion inhibition of mild steel in acidic solution by some oxo-triazole derivatives. Corros Sci 51: 2588–2595
50. Ali SA, Al-Muallem HA, Saeed MT et al (2008) Hydrophobic-tailed bicycloisoxazolidines: a comparative study of the newly synthesized compounds on the inhibition of mild steel corrosion in hydrochloric and sulfuric acid media. Corros Sci 50:664–675
51. Li W, He Q, Pei C et al (2007) Experimental and theoretical investigation of the adsorption behaviour of new triazole derivatives as inhibitors for mild steel corrosion in acid media. Electrochim Acta 52:6386–6394

52. Manivel A, Ramkumar S, Wu JJ et al (2014) Exploration of (*S*)-4,5,6,7-tetrahydrobenzo [*d*] thiazole-2,6-diamine as feasible corrosion inhibitor for mild steel in acidic media. J Environ Chem Eng 2:463–470
53. Hassan HH, Abdelghani E, Amin MA (2007) Inhibition of mild steel corrosion in hydrochloric acid solution by triazole derivatives: part I. Polarization and EIS studies. Electrochim Acta 52:6359–6366
54. Markhali BP, Naderi R, Mahdavian M et al (2013) Electrochemical impedance spectroscopy and electrochemical noise measurements as tools to evaluate corrosion inhibition of azole compounds on stainless steel in acidic media. Corros Sci 75:269–279
55. Ali SA, Al-Muallem HA, Rahman SU et al (2008) Bis-isoxazolidines: a new class of corrosion inhibitors of mild steel in acidic media. Corros Sci 50:3070–3077
56. Abboud Y, Abourriche A, Saffaj T et al (2006) The inhibition of mild steel corrosion in acidic medium by 2,2′-bis (benzimidazole). Appl Surf Sci 252:8178–8184
57. Dhayabaran VV, Lydia IS, Merlin JP et al (2004) Inhibition of corrosion of commercial mild steel in presence of tetrazole derivatives in acid medium. Ionics 10:123–125
58. Tansug G, Tuken T, Kicir N et al (2014) Investigation of 2-aminoethanethiol as corrosion inhibitor for steel using response surface methodology (RSM). Ionics 20:287–294
59. Kesavan D, Tamizh MM, Gopiraman M et al (2012) Physicochemical studies of 4-substituted *N*-(2-mercaptophenyl)-salicylideneimines: corrosion inhibition of mild steel in an acid medium. J Surfact Deterg 15:567–576
60. Al-Amiery AA, Kadhum AAH, Mohamad AB et al (2013) A novel hydrazinecarbothioamide as a potential corrosion inhibitor for mild steel in HCl. Materials 6:1420–1431
61. Popova A, Christov M, Zwetanova A (2007) Effect of the molecular structure on the inhibitor properties of azoles on mild steel corrosion in 1 M hydrochloric acid. Corros Sci 49:2131–2143
62. Popova A, Christov M (2006) Evaluation of impedance measurements on mild steel corrosion in acid media in the presence of heterocyclic compounds. Corros Sci 48:3208–3221
63. Tang Y, Zhang F, Hu S et al (2013) Novel benzimidazole derivatives as corrosion inhibitors of mild steel in the acidic media. Part I: gravimetric, electrochemical, SEM and XPS studies. Corros Sci 74: 271–282
64. Ashassi-Sorkhabi H, Seifzadeh D, Hosseini MG (2008) EN, EIS and polarization studies to evaluate the inhibition effect of 3H-phenothiazin-3-one, 7-dimethylamin on mild steel corrosion in 1 M HCl solution. Corros Sci 50:3363–3370
65. Saliyan VR, Adhikari AV (2008) Quinolin-5-ylmethylene-3-{[8-(trifluoromethyl) quinolin-4-yl] thio} propanohydrazide as an effective inhibitor of mild steel corrosion in HCl solution. Corros Sci 50: 55–61
66. Tüken T, Demir F, Kıcır N et al (2012) Inhibition effect of 1-ethyl-3-methylimidazolium dicyanamide against steel corrosion. Corros Sci 59:110–118
67. El-Rehim SSA, Refaey SAM, Taha F et al (2001) Corrosion inhibition of mild steel in acidic medium using 2-amino thiophenol and 2-cyanomethyl benzothiazole. J Appl Electrochem 31:429–435
68. Kabel KI, Zakaria K, Abbas MA, Khamis EA (2014) Assessment of corrosion inhibitive behavior of 2-aminothiophenol derivatives on carbon steel in 1 M HCl. J. Ind. Eng. Chem. in press
69. Kosari A, Momeni M, Parvizi R et al (2011) Theoretical and electrochemical assessment of inhibitive behavior of some thiophenol derivatives on mild steel in HCl. Corros Sci 53:3058–3067
70. Wang IS (2007) Corrosion research trends. Nova Science, New York
71. Tansuğ G, Tüken T, Giray ES et al (2014) A new corrosion inhibitor for copper protection. Corros Sci 84:21–29
72. Bockris J, Reddy AKN, Gamboa-Aldeco M (2000) Modern electrochemistry, vol 2A. Kluwer Academic/Plenum, New York
73. Hsu CH, Mansfeld F (2001) Technical note: concerning the conversation of the constant phase element parameter Y0 into a capacitance. Corrosion 57:747–748
74. Lemlein R (1973) Diplomarbeit, Institut fur Physikalische Chemie und Electrochemie III der Universitat (TH) Karlsruhe, Germany
75. Lorenz WJ (1965) Der einfluss von halogenidionen auf die anodische auflosung des eisens. Corros Sci 5:121–131
76. Darwish NA, Hilbert F, Lorenz WJ et al (1973) The influence of chloride ions on the kinetics of iron dissolution. Electrochim Acta 18: 421–425